S1. Supplementary methods:

S1.1. Forward modeled 'pseudocoral'- observed coral comparisons

To assess the ability of each pseudocoral network to capture the patterns of variability in the observed coral network, we compared the spatial and temporal pattern of ENSO and the trend. First, we obtained the spatial expression of the significant modes of $\delta^{18}O$ variability by correlating the PCs with the SST and SSS fields. We then regressed the linear trend onto the fields to determine the magnitude of the trend (in °C/year and PSU/year) throughout the Indo-Pacific. We calculated the root mean square error (RMSE) between the observed and pseudocoral correlation and regression fields as:

$$\sqrt{\left(\sum_{i=1}^{N}(coeff_{(obs)i} - coeff_{(pseudo)i})^2\right)/N}, \qquad \text{(S1)},$$

where coeff represents the correlation coefficient (r) or regression coefficient (β) over N grid boxes indexed by *i*. In each case, we projected the ENSO PC and linear trend onto the corresponding SST and SSS fields, with ERSSTv2-SST and SODA-SSS used as default fields for the other variable in SST or SSS only pseudocoral networks. Second, to determine whether the psuedocorals captured the temporal evolution of ENSO and the trend observed in the corals, we regressed the pseudocoral PCs on the observed PCs. If the pseudocorals captured the evolution of ENSO and the trend through time, a significant relationship with a slope near unity would be expected. Finally, we used an analysis of covariance [*Zar*, 1999] to compare the slope of the shared linear trend in the observed and pseudocoral networks (‰ per decade). To address whether differences in the magnitude of the trend could be attributed to discrepancies in certain regions of the tropical Indo-Pacific, we also compared the magnitude of the trend slope at each coral site. A simple t-test was used to determine if the mean difference between the observed and pseudocoral trend at the 23 sites was significantly different from zero.

S1.2. Mean state and ENSO-related variance

We compare 20th-century trends in mean state and ENSO-related variance, following an approach similar to that of *Meehl et al*. [2007] [after *van Oldenborgh et al*., 2005; *Yamaguchi and Noda,* 2006]. First, we high-pass filtered the ENSO PC by convoluting an 11-year normalized hamming window with the ENSO PC to isolate the interannual variance. Because this filtering process removes 5 years from either end of the record, the following analyses were performed between 1895 and 1985. We determined the spatial expression of ENSO and the trend at the coral sites by regressing the high-pass filtered ENSO PC and linear trend onto the observed or pseudocoral records at the 23 coral sites. We calculated the mean state change in the tropical Pacific (x-axis) as the correlation between the ENSO and linear trend regression coefficients at the 14 Pacific coral sites (80ºW-120ºE). A positive correlation coefficient indicates spatial similarity between the trend and the ENSO pattern and is thus referred to as an "El Niño-like" trend [after *Meehl et al.,* 2007]. Note that this terminology is used only to refer to the spatial pattern of the trend, with no inferences for the underlying dynamics. Finally, we calculated the change in ENSO variability (y-axis) as the ratio of the standard deviation of the high-pass filtered ENSO PC in the last 45 years (1941-1985) to the standard deviation of the filtered ENSO PC in the first 45 years (1895-1939) of the analysis. A ratio of 1 indicates that there was no change in the standard deviation of the ENSO PC (ENSO-related variance) between the first and last 45 years of the analysis.

To assess the sensitivity of the ENSO-related variance and mean state trends to the underlying network and time period covered by the analysis, we performed sensitivity analyses by randomly selecting subsets from the original data set. First, we randomly selected thirty years from the first and last 45 years of the high-pass filtered ENSO PC and calculated the standard

deviation ratio (y-axis) for each subset. We then assessed the sensitivity of the mean state trend to the underlying network of coral sites by randomly selecting twenty sites from the full 23-site network for SVD analysis. For each subset, we selected the ENSO and trend PCs from the consecutive leading significant principal components (PCs 1-3) and the mean state trend was calculated as above. We defined the trend as the PC that displayed the greatest slope (β) when regressed on time, and ENSO as the remaining PC that displayed the strongest relationship with (instrumental or modeled) Nino 3.4 SSTs. We excluded the subset from the mean state calculation if ENSO and the trend were not separated into independent PCs (observed in a few GFDL cm2.1 subsets). We performed further sensitivity tests by varying the number of subsets analyzed (between 10 and 1000), by performing the variance calculation on the full 100-year period (before filtering the ENSO PC), by varying hamming window length, and by changing the criteria for selection of the PCs (e.g., the number considered, statistics for selection, and whether significance was required). Varying these input criteria did not influence the interpretation of the results. Therefore, we selected the most conservative approach, where significance of the PCs was required, the ENSO PC was filtered with an 11-year normalized hamming window to maintain only variability up to 10 years, and the largest number of subsets that maintained independence of the samples was used to quantify sensitivity (1000 subsets of time and 50 subsets of sites).

Table S1: Slope of the $\delta^{18}O_{sw}$-salinity relationship (‰/PSU, from LeGrande and Schmidt 2006) for the regions containing coral records used in this analysis [*Ault et al*., 2009].

Region	Latitudes	Longitudes	Slope (+/- σ)
Tropical Pacific	**5S to 13N**	**70W to 120E**	**0.27 (+/- 0.006)**
Chiriqui, Panama	7ºN	82ºW	Linsley et al., 1994
Urvina Bay, Galapagos	0ºS	91ºW	Dunbar et al., 1994
Jarvis Island	0ºS	160ºW	Tudhope et al., unpublished data
Maiana Atoll, Kiribati	0ºN	173ºE	Urban et al., 2000
Double Reef, Guam	13ºN	144ºE	Asami et al., 2005
Bunaken Island, Indonesia	1ºN	124ºE	Charles et al., 2003
South Pacific	**5S to 28S**	**70W to 113E**	**0.45 (+/- 0.028)**
Moorea, French Polynesia	17ºS	149ºW	Boiseau et al., 1998
Rarotonga, Cook Islands	21ºS	159ºW	Linsley et al., 2000
Palmerston, Cook Islands	18ºS	163ºW	Tudhope et al., unpublished data
Savusavu Bay, Fiji	17ºS	178ºE	Bagnato et al., 2005
Espiritu Santo, Vanuato	15ºS	167ºE	Quinn et al., 1996
New Caledonia	22ºS	166ºE	Quinn et al., 1998
Abraham Reef, Australia	22ºS	153ºE	Druffel and Griffin, 1999
Bramble Cay, Papua New Guinea	9ºS	144ºE	Cole, unpublished data
Houtman Abrolhos, Australia	28ºS	113ºE	Kuhnert et al., 1999
Indian Ocean	**23S to 20N**	**120E to 38E**	**0.16 (+/- 0.004)**
Bali, Indonesia	8ºS	115ºE	Charles et al., 2003
Mahe, Seychelles	4ºS	55ºE	Charles et al., 1997
Mentawai, Sumatra	2ºS	99ºE	Abram et al., 2008
La Reunión	21ºS	55ºE	Pfeiffer et al., 2004
Ifaty, Madagascar	23ºS	43ºE	Zinke et al., 2004
Malindi, Kenya	3ºS	40ºE	Cole et al., 2000
Tutia, Tanzania	8ºS	39ºE	Barnett, 2006; Barnett et al., unpublished data
Zanzibar, Tanzania	6ºS	39ºE	Barnett, 2006; Barnett et al., unpublished data

Table S2: Statistics for the regression of the observed coral ENSO PC (PC2) and the observed coral trend PC (PC1) with the pseudocoral ENSO and trend PCs, where bold indicates significance at the 95% confidence level and bold italics represents significance at the 99% confidence level.

Pseudocoral network input datasets		**% variance explained**		**R^2**		**F**		**P**		**slope**	
SST	SSS	***ENSO***	***Trend***	***ENSO***	***Trend***	***ENSO***	***Trend***	***ENSO***	***Trend***	***ENSO***	***Trend***
ERSSTv2	SODA	51.4%	14.9%	***0.497***	***0.445***	***30.7***	***24.8***	***<0.001***	***<0.001***	***0.667***	***0.862***
ERSSTv2	CartonGOA	53.6%	16.6%	***0.488***	***0.317***	***29.5***	***14.4***	***<0.001***	***<0.001***	***0.701***	***0.751***
ERSSTv3	SODA	51.7%	14.2%	***0.487***	***0.444***	***29.5***	***24.7***	***<0.001***	***<0.001***	***0.651***	***0.871***
HadISST	SODA	47.2%	14.4%	***0.427***	***0.365***	***23.1***	***17.8***	***<0.001***	***<0.001***	***0.605***	***0.743***
Kaplan ext.v2	SODA	44.1%	14.3%	***0.457***	***0.650***	***26.1***	***57.6***	***<0.001***	***<0.001***	***0.695***	***1.07***
ERSSTv2		52.7%	17.9%	***0.474***	***0.333***	***27.9***	***15.5***	***<0.001***	***<0.001***	***0.788***	***0.833***
ERSSTv3		52.9%	16.9%	***0.464***	**0.272**	***26.7***	**11.6**	***<0.001***	**0.0018**	***0.766***	**0.763**
HadISST		47.6%	17.3%	***0.375***	***0.344***	***18.6***	***16.3***	***<0.001***	***<0.001***	***0.688***	***0.802***
Kaplan ext.v2		42.0%	18.7%	***0.438***	***0.400***	***24.1***	***20.7***	***<0.001***	***<0.001***	***0.824***	***0.869***
	SODA	40.1%	40.1%	***0.433***	**0.148**	***23.7***	**5.37**	***<0.001***	**0.0272**	***1.80***	**0.772**
	CartonGOA	20.1%	44.2%	0.0435	0.115	1.41	4.02	0.244	0.0538	1.61	1.29

Table S3: Root mean square error (RMSE) between the observed and pseudocoral ENSO correlation fields, calculated as:

$$\sqrt{\left(\sum_{i=1}^{N}(coeff_{(obs)i} - coeff_{(pseudo)i})^2\right)/N}$$

, where coeff represents the correlation coefficient (r) and N is the number of grid boxes (i). In each case, the ENSO PC was projected onto the SST and SSS fields corresponding to the input for the pseudocoral network, with ERSSTv2-SST and SODA-SSS used as default fields for the other variable in SST or SSS only pseudocoral networks. Values in bold indicate RMSEs which were less than the 950th lowest RMSE of 1000 random time series correlated with the underlying SST or SSS field (i.e., the two fields were not significantly different at the 95% CI).

Pseudocoral network input datasets		**ENSO PC-SST RMSE**	**ENSO PC-SSS RMSE**
SST	SSS		
ERSSTv2	SODA	**0.211**	**0.224**
ERSSTv2	CartonGOA	**0.202**	**0.222**
ERSSTv3	SODA	**0.221**	**0.231**
HadISST &	SODA	0.232	0.260
Kaplan ext.v2	SODA	**0.232**	0.246
ERSSTv2		**0.202**	**0.231**
ERSSTv3		**0.215**	**0.238**
HadISST		0.316	0.382
Kaplan ext.v2		**0.232**	0.253
	SODA	**0.237**	**0.180**
	CartonGOA	0.302	0.415

Figure S1. (a) Correlation of the ENSO PC observed in corals over the 1958-1990 period (b, black) with the $\delta^{18}O_{coral}$ record from each coral site. (c) Same as in (a) but for the high-pass filtered ENSO PC from corals over the 1890-1990 period (d). (e) Regression coefficient from the regression of the $\delta^{18}O_{coral}$ records with the linear trend over the 1958-1990 period, estimated from linear regression of the trend PC (f). (g) Same as in (e) but for the linear trend over the 1890-1990 period (h). The ENSO PC (b) and linear trend (f) from pseudocorals modeled with both SST and SSS are shown in gray for comparison.

Figure S2. (left) Correlation of SST and SSS and (right) the SSS trend (PSU per decade) between 1958 and 1990 over the tropical Indo-Pacific in (a) Observational SST and SSS: ERSSTv2 and SODA, (b) GFDL cm 2.0, (c) GFDL cm 2.1, (d) NCAR CCSM3, (e) NCAR PCM1, (f) GISS eh, (g) GISS er, and (h) HadCM3. Only significant correlations and trends are shown.

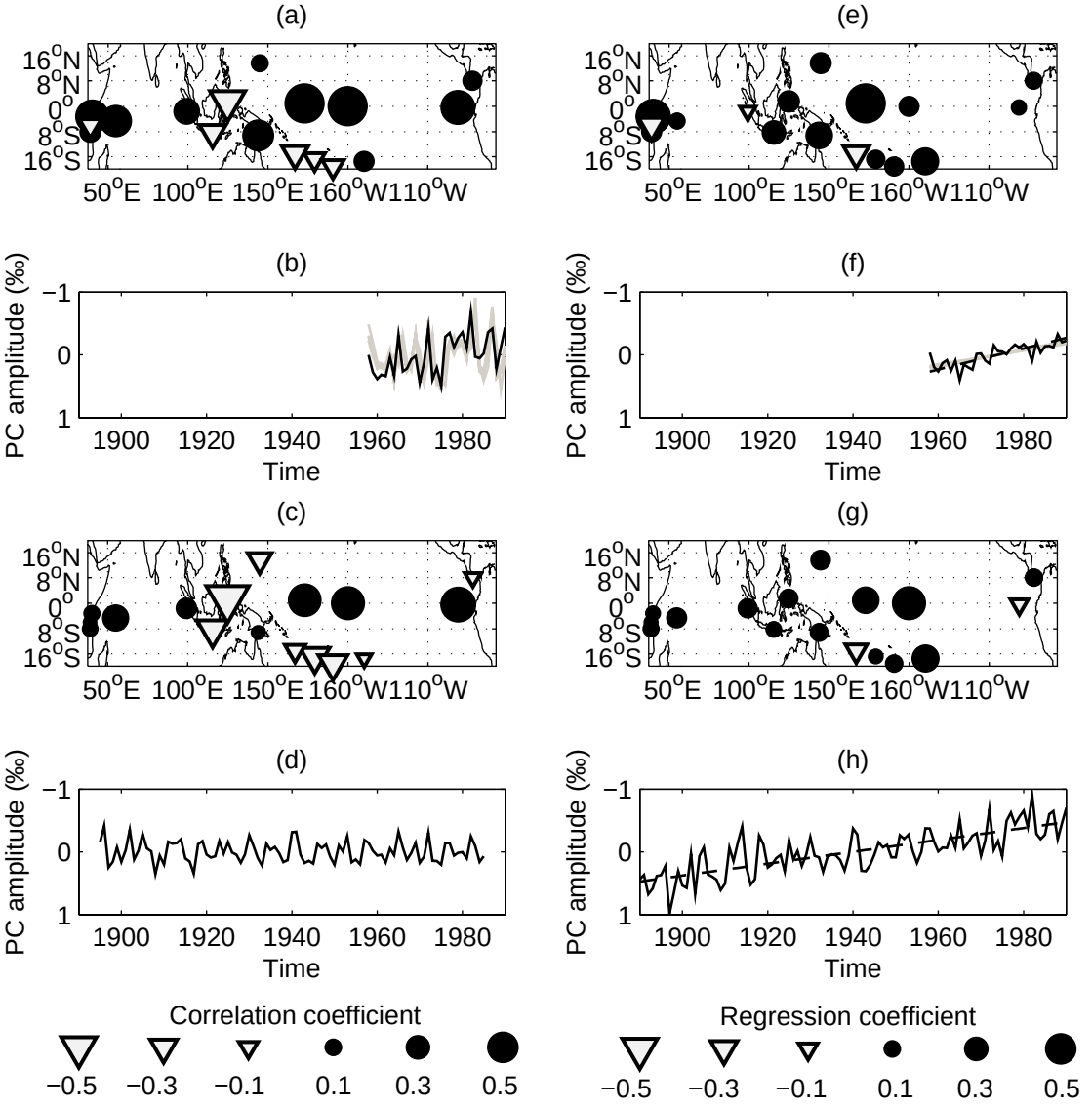
(a)
(e)
16°N
8°N
0°
8°S
16°S
50°E 100°E 150°E 160°W 110°W
(b)
(f)
PC amplitude (‰)
−1
0
1
1900 1920 1940 1960 1980
Time
(c)
(g)
(d)
(h)
Correlation coefficient
−0.5 −0.3 −0.1 0.1 0.3 0.5
Regression coefficient
−0.5 −0.3 −0.1 0.1 0.3 0.5

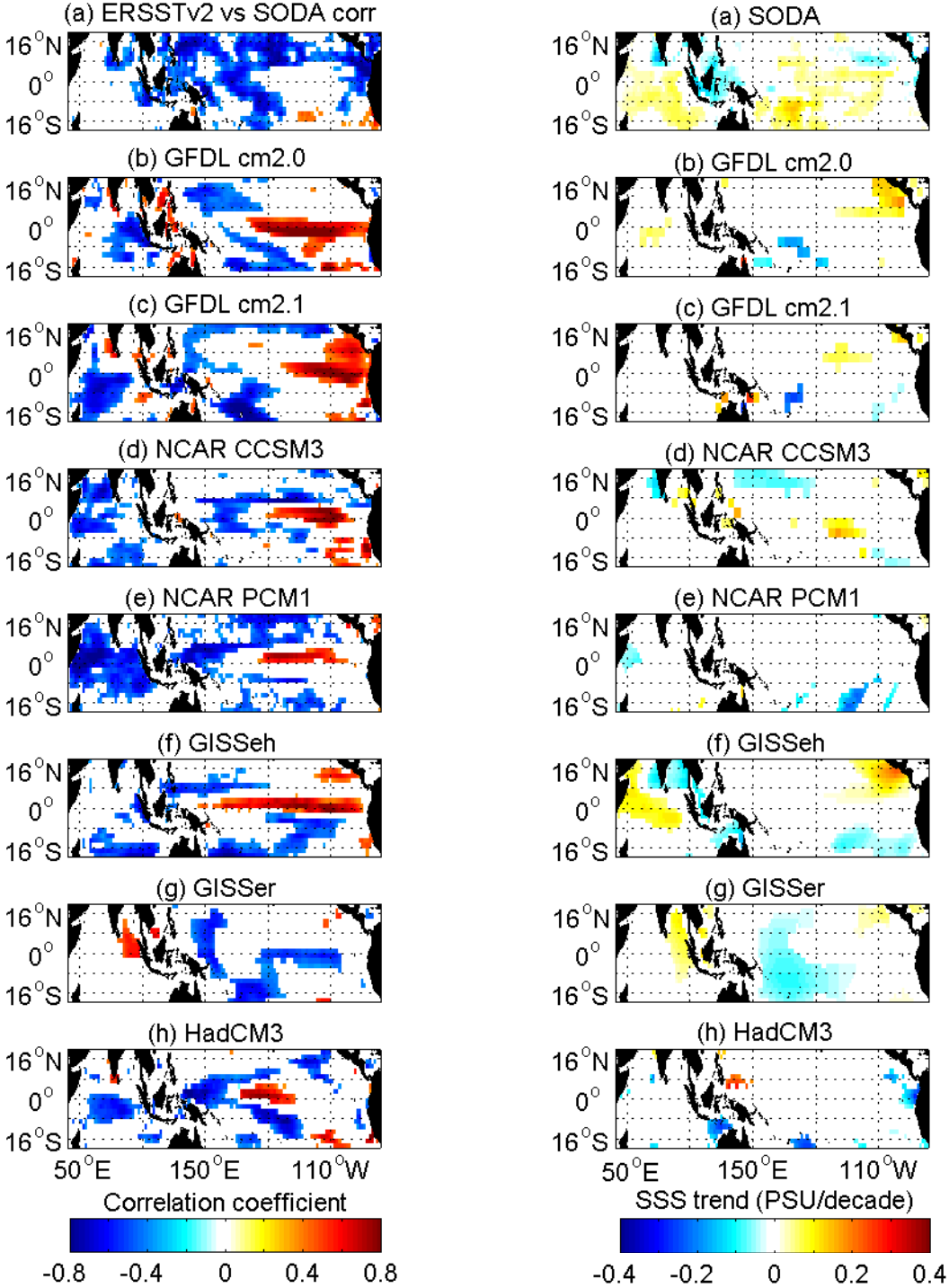
(a) ERSSTv2 vs SODA corr
(b) GFDL cm2.0
(c) GFDL cm2.1
(d) NCAR CCSM3
(e) NCAR PCM1
(f) GISSeh
(g) GISSer
(h) HadCM3
16°N
0°
16°S
50°E
150°E
110°W
Correlation coefficient
-0.8
-0.4
0
0.4
0.8
(a) SODA
(b) GFDL cm2.0
(c) GFDL cm2.1
(d) NCAR CCSM3
(e) NCAR PCM1
(f) GISSeh
(g) GISSer
(h) HadCM3
SSS trend (PSU/decade)
-0.4
-0.2
0
0.2
0.4

Supplemental references.

Abram, N.J. et al. (2008) Recent intensification of tropical climate variability in the Indian Ocean, *Nature Geosciences*, doi:10.1038/ngeo357.

Asami, R., et al. (2005), Interannual and decadal variability of the western Pacific sea surface condition for the years 1787-2000: Reconstruction based on stable isotope record from a Guam coral, *J. Geophys. Res. Oceans*, *110*(C5), doi:10.1029/2004JC002555.

Bagnato, S., et al. (2005), Coral oxygen isotope records of interdecadal climate variations in the South Pacific Convergence Zone region, *Geochemistry Geophysics Geosystems*, *6*, doi:10.1029/2004GC000879.

Barnett H.R., (2006), 20th Century climate variability in the tropical Indian ocean from a new network of coral oxygen isotope chronologies, M.S., Dept. of Geosciences, University of Arizona.

Boiseau, M., et al. (1998), Atmospheric and oceanic evidences of El Niño Southern scillation events in the south central Pacific Ocean from coral stable isotopic records over the last 137 years, *Paleoceanography*, *13*(6), 671-685.

Charles, C. D., et al. (1997), Interaction between the ENSO and the Asian monsoon in a coral record of tropical climate, *Science*, *277*(5328), 925-928.

Charles, C.D., et al. (2003), Monsoon-tropical ocean interaction in a network of coral records spanning the 20th century, *Marine Geology*, *201*, 207-222.

Cole, J. E., et al. (2000), Tropical Pacific forcing of decadal SST variability in the western Indian Ocean over the past two centuries, *Science*, *287*(5453), 617-619.

Druffel, E. R. M., and S. Griffin (1999), Variability of surface ocean radiocarbon and stable isotopes in the southwestern Pacific, *J. Geophys. Res. Oceans*, *104*(C10), 23607-23613.

Dunbar, R.B., et al. (1994), Eastern Pacific Sea Surface Temperature since 1600 A.D.: The d18O Record of Climate Variability in Galapagos Corals, *Paleoceanography*, *9*, 291-315.

Kuhnert, H., et al. (1999), A 200-year coral stable oxygen isotope record from a high-latitude reef off western Australia, *Coral Reefs*, *18*(1), 1-12.

Linsley, B. K., et al. (1994), A coral-based reconstruction of intertropical convergence zone variability over Central America since 1707, *J. Geophys. Res. Oceans*, *99*(C5), 9977-9994.

Linsley, B. K., et al. (2000), Decadal sea surface temperature variability in the subtropical South Pacific from 1726 to 1997 AD, *Science*, *290*(5494), 1145-1148.

Pfeiffer, M., et al. (2004), Oceanic forcing of interannual and multidecadal climate variability in the southwestern Indian Ocean: Evidence from a 160 year coral isotopic record (La Reunion, 55 degrees E, 21 degrees S), *Paleoceanography*, *19*(4), doi:10.1029/2003PA000964.

Quinn, T. M., et al. (1996), New stable isotope results from a 173-year coral from Espiritu Santo, Vanuatu, *Geophys. Res. Lett.*, *23*(23), 3413-3416.

Quinn, T. M., et al. (1998), A multicentury stable isotope record from a New Caledonia coral: Interannual and decadal sea surface temperature variability in the southwest Pacific since 1657 AD, *Paleoceanography*, *13*(4), 412-426.

Urban, F. E., J. E. Cole, and J. T. Overpeck (2000), Influence of mean climate change on climate variability from a 155-year tropical Pacific coral record, *Nature*, *407*(6807), 989–993.

van Oldenborgh, G.J., S.Y. Philip, and M. Collins (2005), El Niño in a changing climate: a multi-model study, *Ocean Sci.*, *1*, 81–95.

Yamaguchi, K., and A. Noda (2006), Global warming patterns over the North Pacific: ENSO vs. AO, *J. Meteorol. Soc. Jpn.*, *84*(1), 221– 241, doi:10.2151/jmsj.84.221.

Zar, J.H. (1999), Comparing Simple Linear Regression Equations, in *Biostatistical analysis*, 4th ed., pp. 360-376, Prentice Hall, Upper Saddle River, New Jersey.

Zinke, J., et al. (2004), ENSO and Indian Ocean subtropical dipole variability is recorded in a coral record off southwest Madagascar for the period 1659 to 1995, *Earth Planet. Sci. Lett.*, *228*(1-2), 177-194.